Intramolecular photochemical electron transfer. 7. Temperature of electron-transfer rates in covalently linked porphyrin-amide-quinone molecules

ARTICLE *in* THE JOURNAL OF PHYSICAL CHEMISTRY · FEBRUARY 1992

Impact Factor: 2.78 · DOI: 10.1021/j100183a041

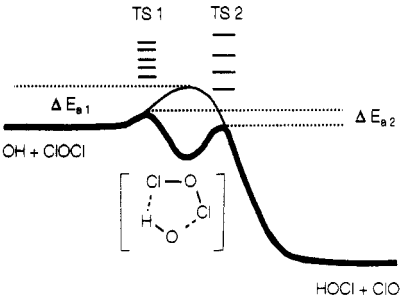

Figure 12. Schematic potential-energy surface (heavy curve) for the OH + ClOCl → products reaction showing the effect of a stable HOClOCl intermediate on the barrier to reaction. The presence of this intermediate results in a lower reaction barrier (ΔE_{a2}) relative to the barrier defined by the X + ClOCl surface for the other reactions in the series (ΔE_{a1}). The observed negative activation energy for this reaction implies two distinct transition states, with the second transition state tighter and more stable than the first (see text).

ClOOCl reaction may also proceed via a stable OH·ClOOCl intermediate, similar to the OH·ClOCl intermediate proposed here:

$$OH + ClOOCl \rightarrow (HO{\cdot}ClOOCl)^* \rightarrow HOCl + ClOO \qquad \Delta H^\circ_{298} = -36 \text{ kcal/mol}$$

Thus the rate constant for OH + ClOOCl reaction may also exhibit a negative temperature dependence. The question becomes whether this large rate constant for the OH + ClOOCl reaction results in a rate at antarctic temperatures which competes with the photolysis rate of ClOOCl. A fast rate for the OH + ClOOCl reaction would shift the catalytic destruction of ozone from one involving ClO dimer photolysis (mechanism I) to one involving HOCl photolysis (mechanism II).

In order to determine what effect the OH + ClOOCl reaction might have on mechanisms of ozone destruction, the OH + ClOCl rate constant was used in a zero-dimensional photochemical kinetic simulation[42] as a surrogate for the rate constant for the OH + ClOOCl reaction. The model was run from 25 August to 1 September, at 65°S, 20 km, and 210 K. The initial conditions simulated the antarctic stratosphere just prior to destruction of ozone; preprocessed air (where NO_x is removed by heterogeneous reactions with polar stratospheric clouds), with elevated concentrations of ClO_x ([ClO] + [ClOOCl] = 3×10^9 cm^{-3}), and midlatitude concentrations of HO_x ([OH] and [HO_2] = 1×10^6 cm^{-3}).

The results of the model reveal that, with midlatitude values of HO_x, the OH + ClOOCl reactions is over 200 times slower than the photolysis of ClOOCl and, as a result, has no significant effect on calculated ozone destruction rates. However, confirmation of these results awaits the direct measurement of the OH + ClOOCl reaction rate constant, and in situ measurements of HO_x in the antarctic stratosphere. If the polar concentrations of HO_x were significantly higher, the OH + ClOOCl reaction may begin to compete with the photolysis of the ClO dimer. The OH + ClOOCl reaction would begin to slowly partition active chlorine from ClOOCl to HOCl, and the destruction of ozone would become limited by HOCl photolysis. The overall rate of the OH + ClOOCl → HOCl + ClOO reaction is, however, constrained by observations of HOCl abundances.[43]

Acknowledgment. We thank P. O. Wennberg for experimental assistance and S. A. Lloyd and D. E. Anderson for use of their photochemical model and acknowledge helpful discussions with W. H. Brune. This work was supported by the National Science Foundation, Grant ATM-8601126.

Registry No. COCl, 7791-21-1; Br, 10097-32-2; Cl, 22537-15-1; F, 14762-94-8; O, 17778-80-2; N, 17778-88-0; OH, 3352-57-6.

(42) Anderson, D. E.; Lloyd, S. A. *J. Geophys. Res.* **1990**, *95*, 7429.
(43) Toon, G. C.; Farmer, C. B. *Geophys. Res. Lett.* **1989**, *16*, 1375.

Intramolecular Photochemical Electron Transfer. 7. Temperature Dependence of Electron-Transfer Rates in Covalently Linked Porphyrin–Amide–Quinone Molecules[1]

Jing-yao Liu and James R. Bolton*

Photochemistry Unit, Department of Chemistry, The University of Western Ontario, London, Ontario, Canada N6A 5B7 *(Received: May 8, 1991; In Final Form: October 14, 1991)*

Intramolecular rate constants k_{ET} for electron transfer (ET) from a porphyrin excited singlet S_1 state to a linked quinone acceptor have been measured as a function of temperature in several solvents for the molecule PAQ [5,10,15-tritolyl-15-(4-carboxylphenyl)porphine linked to *p*-benzoquinone via an amide group]. Most of the data could be analyzed successfully using the high-temperature form of the semiclassical Marcus equation. The analysis of temperature dependence data allows the separation of the electronic and nuclear factors in the Marcus equation. The results indicate that both factors are solvent dependent. The electronic factor, involving the electronic coupling energy H_{rp}, is found to have larger values in polar solvents and smaller values in most nonpolar solvents. On the other hand, the nuclear factor is not found to correlate with solvent polarity. The analysis of the temperature dependence of k_{ET} provides a plausible explanation for the scatter found in a former analysis of solvent effects for photoinduced electron transfer in PAQ.

Introduction

Electron transfer (ET) reactions[2] are among the most common and fundamental processes in chemistry and biochemistry. Since the development of the theory of electron transfer by Marcus and others,[3-5] this subject has been an area of lively investigation. In particular, over the past 12–14 years there has been a growing interest in the study of intramolecular ET in molecules where a donor and an acceptor are covalently linked; these systems have proved to be a fruitful testing ground for systems designed to mimic

(1) Contribution No. 441, Photochemistry Unit, Department of Chemistry, The University of Western Ontario.
(2) For reviews, see: (a) Sutin, N.; Marcus, R. A. *Biochim. Biophys. Acta* **1985**, *811*, 265. (b) Bolton, J. R.; Archer, M. D. In *Electron Transfer in Inorganic, Organic and Biological Systems*; Bolton, J. R., Mataga, N., McLendon, G. L., Eds.; Advances in Chemistry Series 228; American Chemical Society: Washington, DC, 1991; Chapter 2, pp 7-23.
(3) Marcus, R. A. (a) *J. Chem. Phys.* **1956**, *24*, 966; (b) *Faraday Discuss. Chem. Soc.* **1960**, *29*, 21; (c) *Annu. Rev. Phys. Chem.* **1964**, *15*, 155; (d) *J. Chem. Phys.* **1965**, *43*, 679.
(4) Levich, V. G.; Dogonadze, R. R. *Collect. Czech. Chem. Commun.* **1961**, *26*, 193.
(5) Kestner, N. R.; Lofan, J.; Jortner, J. *J. Phys. Chem.* **1974**, *78*, 2148.

0022-3654/92/2096-1718$03.00/0

the in vivo ET processes in photosynthesis.[6]

Many factors can influence ET rate constants. These include overall Gibbs energy of reaction; distance between the donor and acceptor moieties, relative orientation of the donor and acceptor, molecular nature of the bridging group, solvent, and temperature.[6] In this paper we shall focus on the temperature dependence of ET rate constants.[7]

Unusual temperature dependence of intramolecular ET rate constants was first demonstrated by Chance and Nishimura,[8] who observed that one of the cytochromes of the photosynthetic bacterium *Chromatium* became oxidized at 77 K following light absorption by the reaction-center bacteriochlorophyll. DeVault and Chance[9] extended this initial observation by showing that below ~150 K the rate of this ET reaction is essentially temperature independent, which indicates that nuclear tunneling mechanisms are likely operating. This behavior was also observed by Arnold and Clayton[10] for the back ET reaction in chromatophore membranes of the photosynthetic bacterium *Rhodopseudomonas sphaeroides*, where the reaction proceeds at almost the same rate from ~100 K down to 1 K.

Heitele et al.[11] have measured the temperature dependence of intramolecular ET in several solvents for molecules where anthracene is linked to dimethylaniline via a polymethylene bridge. They found that plots of ln k_{ET} vs $1/T$ are curved. Recently O'Driscoll et al.[12] showed by calculation that the temperature dependence of ET reactions can be Arrhenius, non-Arrhenius, or temperature independent according to the $\Delta G°$ values.

Delaney et al.[13] measured intramolecular ET in a capped zinc porphyrin–quinone molecule in 21 solvents over the temperature range 80–300 K. They found a weak temperature and solvent dependence of k_{ET} and ascribed this to a nonadiabatic electron tunneling mechanism.

Liang et al.[14] have measured the temperature dependence of charge-shift ET reactions where an electron moves from a biphenyl moiety to an acceptor across a rigid steroid (5α-androstane). When the acceptor is such that the ET reaction is in the "normal region" of Marcus theory, they find that the ET rate constants decrease as the temperature is lowered; however, if the acceptor is such that the ET reaction is strongly into the "inverted region", they observe that the ET rate constants are almost temperature independent, which they ascribed to a dominance of nuclear tunneling in the ET mechanism.

Over the past several years we have studied photoinduced ET in a series of linked donor–acceptor molecules in which a porphine [5,10,15-tritolyl-15-(4-carboxylphenyl)] is linked to *p*-benzoquinone via various amide linkages.[15-21] The ET rate constants

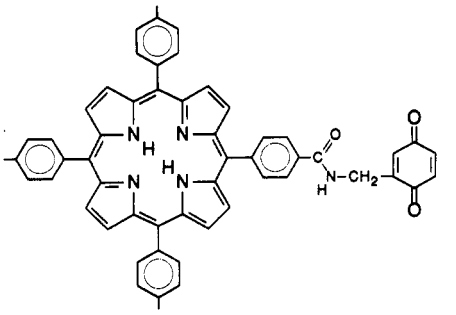

PAQ

in one of these molecules (PAQ) have been examined at 295 K in considerable detail,[17-21] since they were found to be very solvent dependent.[17,19-21] Although the results conformed reasonably well with the predictions of Marcus theory, there was considerable scatter in the correlation.[20] In this paper we examine the possible origin of this scatter via a careful study of the temperature dependence of photoinduced ET in PAQ for several solvents.

Theory

According to Marcus theory,[2] the ET rate for a nonadiabatic reaction constant can be expressed as[3-5]

$$k_{ET} = \kappa_{el}\nu_n\kappa_n = \frac{2\pi}{\hbar}\frac{H_{rp}^2}{(4\pi\lambda k_B T)^{1/2}}\exp\left[-\frac{\Delta G^*}{k_B T}\right] \quad (1)$$

where

$$\kappa_{el}\nu_n = \frac{2\pi}{\hbar}\frac{H_{rp}^2}{(4\pi\lambda k_B T)^{1/2}};\quad \kappa_n = \exp\left[-\frac{\Delta G^*}{k_B T}\right];$$

$$\Delta G^* = \frac{(\Delta G° + \lambda)^2}{4\lambda}$$

κ_{el} and κ_n are the electronic and nuclear factors; ν_n is the frequency of nuclear motion through the transition state (usually taken as $k_B T/h$); k_B is the Boltzmann constant; ΔG^* is the Gibbs activation energy in Marcus theory; and $\Delta G°$ is the Gibbs energy change (driving force) for the ET reaction. H_{rp} is the electronic coupling matrix element for the reactants (R) and products (P), where R ≡ PAQ and P ≡ $P^{\bullet+}AQ^{\bullet-}$.

$$H_{rp} = \langle \psi_R° | \hat{\mathcal{H}}_{el} | \psi_P° \rangle \quad (2)$$

Here $\psi_R°$ and $\psi_P°$ are the electronic wave functions of the equilibrium reactant and product states, respectively, and $\hat{\mathcal{H}}_{el}$ is the Born–Oppenheimer (rigid nuclear coordinates) electronic Hamiltonian for the system. H_{rp} is determined in part by the distance between the electron donor and the electron acceptor and in part by the nature of the bridging group.[21,22] λ is the Gibbs reorganization energy of the reaction. Equation 1 is valid as long as the ET reaction is in the "normal" region; in the "inverted" region more complex expressions must be used.[2b] Indeed Liang et al.[14] have shown that eq 1 is adequate in the normal region but

(6) For a recent review of this area see: Connolly, J. S.; Bolton, J. R., Intramolecular electron transfer: history and some implications for artificial photosynthesis. In *Photoinduced Electron Transfer*; Fox, M. A., Chanon, M., Eds.; Elsevier: New York, 1989; Vol. 4, pp 303–393.

(7) A preliminary account of some of the work described in this paper is contained in a review: Bolton, J. R.; Schmidt, J. A.; Ho, T.-F.; Liu, J.-Y.; Roach, K. J.; Weedon, A. C.; Archer, M. D.; Wilford, J. H.; Gadzekpo, V. P. Y. In *Electron Transfer in Inorganic, Organic and Biological Systems*; Bolton, J. R., Mataga, N., McLendon, G. L., Eds.; Advances in Chemistry, Series 228; American Chemical Society: Washington, DC, 1991; Chapter 7, pp 117–131.

(8) Chance, B.; Nishimura, M. *Proc. Natl. Acad. Sci. U.S.A.* **1960**, *46*, 19.

(9) DeVault, D.; Chance, B. *Biophys. J.* **1966**, *6*, 825.

(10) Arnold, W.; Clayton, R. K. *Proc. Natl. Acad. Sci. U.S.A.* **1960**, *46*, 769.

(11) Heitele, H.; Finckh, P.; Weeren, S.; Poellinger, F.; Michel-Beyerle, M. E. *J. Phys. Chem.* **1989**, *93*, 5173.

(12) O'Driscoll, E.; Simon, J. D.; Peters, K. S. *J. Am. Chem. Soc.* **1990**, *112*, 7091.

(13) Delaney, J., private communication.

(14) (a) Liang, N.; Miller, J. R.; Closs, G. L. *J. Am. Chem. Soc.* **1989**, *111*, 8740. (b) Liang, N.; Miller, J. R.; Closs, G. L. *J. Am. Chem. Soc.* **1990**, *112*, 5353.

(15) Paper 1 in this series: McIntosh, A. R.; Siemiarczuk, A.; Bolton, J. R.; Stillman, M. J.; Ho, T.-F.; Weedon, A. C. *J. Am. Chem. Soc.* **1983**, *105*, 7215.

(16) Paper 2 in this series: Siemiarczuk, A.; McIntosh, A. R.; Ho, T.-F.; Stillman, M. J.; Roach, K. J.; Weedon, A. C.; Bolton, J. R.; Connolly, J. S. *J. Am. Chem. Soc.* **1983**, *105*, 7224.

(17) Paper 3 in this series; Schmidt, J. A.; Siemiarczuk, A.; Weedon, A. C.; Bolton, J. R. *J. Am. Chem. Soc.* **1985**, *107*, 6112–6114.

(18) Paper 4 in this series; Schmidt, J. A.; McIntosh, A. R.; Weedon, A. C.; Bolton, J. R.; Connolly, J. S.; Hurley, J. K.; Wasielewski, M. R. *J. Am. Chem. Soc.* **1988**, *110*, 1733.

(19) Schmidt, J. A., Ph.D. Thesis, The University of Western Ontario, London, Ontario, Canada, 1986.

(20) Paper 5 in this series: Schmidt, J. A.; Liu, J.-Y.; Bolton, J. R.; Archer, M. D.; Gadzekpo, V. P. Y. *J. Chem. Soc., Faraday Trans. 1* **1989**, *85*, 1027.

(21) Paper 6 in this series: Liu, J.-Y.; Schmidt, J. A.; Bolton, J. R. *J. Phys. Chem.* **1991**, *95*, 6924.

(22) Liu, J.-Y. Ph.D. Thesis, The University of Western Ontario, London, Ontario, Canada, 1991.

does not account for the observed temperature independence of ET in the inverted region.

In eq 1 the electronic factor κ_{el} accounts for the electron-transfer efficiency at the crossing point; the nuclear factor κ_n accounts for the probability of reactants reaching the transition state. These two factors can be separated in studies of the temperature dependence of the reaction. If we assume that the distribution of PAQ molecular conformations does not change very much with temperature, then κ_{el} can be assumed to be almost temperature independent.

The reorganization energy λ is usually divided into an inner-sphere term λ_{in} involving vibrational energy changes between the reactant and product states and an outer-sphere term λ_{out} involving the solvent orientation and polarization[2]

$$\lambda = \lambda_{in} + \lambda_{out} \tag{3}$$

If the reactant complex is assumed to consist of two spheres in a dielectric continuum, λ_{out} is given by

$$\lambda_{out} = \frac{e^2}{4\pi\epsilon_o}\left[\frac{1}{2a_D} + \frac{1}{2a_A} - \frac{1}{r_{DA}}\right]\left[\frac{1}{\epsilon_{op}} - \frac{1}{\epsilon_s}\right] \tag{4a}$$

where a_D and a_A are the radii of the donor and acceptor spheres, r_{DA} is the distance between the centers of the spheres, and ϵ_{op} and ϵ_s are the optical and static dielectric constants of the surrounding medium. Similar expressions are found for other models and it is common to express λ_{out} by the semiempirical expression

$$\lambda_{out} = B\left[\frac{1}{\epsilon_{op}} - \frac{1}{\epsilon_s}\right] \tag{4b}$$

where B is a parameter whose value depends on the model chosen and the molecular dimensions.

After the porphyrin chromophore in PAQ is raised to its first excited singlet state, electron transfer occurs from the porphyrin to the quinone to form a radical ion pair $P^{\bullet+}AQ^{\bullet-}$. ET rate constants are usually obtained from fluorescence lifetimes using the equation[16]

$$k_{ET} = \frac{1}{\tau_1} - \frac{1}{\tau_2} \tag{5}$$

where τ_1 and τ_2 are the fluorescence lifetimes of the porphyrin, respectively, with and without ET quenching. Usually τ_2 is obtained from a molecule of very similar structure, but in which ET does not occur. In our case, τ_2 is the lifetime of the corresponding covalently-linked porphyrin–hydroquinone compound $PAQH_2$.

Experimental Methods

The PAQ and $PAQH_2$ solutions were prepared as described previously.[20,21] The UV spectra of solutions of PAQ and $PAQH_2$ were run before the lifetime measurements were made. The Soret band absorbance in all samples was adjusted to be less than 1.5, so that the concentrations were $\sim 10^{-5}$–10^{-6} M ($\epsilon \cong 5 \times 10^5$ M^{-1} cm^{-1}).

All solvents were first distilled and then stored over freshly dried molecular sieves for more than 24 h. A small piece of potassium carbonate was stored with the chloroform and methylene chloride to neutralize the trace amount of acid that can exist in these solvents. 2-Methyltetrahydrofuran (2-MTHF) was first dried over metallic sodium and then distilled. The fluorescence of the pure solvents under the experimental conditions was first checked and no extra emissions were observed.

Sample solutions were then transferred into 5 mm diameter glass vials and evacuated through several freeze–pump–thaw cycles until the pressure was $<10^{-3}$ Torr; the glass vial was then sealed off with a gas torch.

Samples in methylene chloride, chloroform, and 2-MTHF change color after vacuum sealing in a glass vial; for these solvents the glass vials were simply sealed with a rubber stopper, the stoppers were first rinsed with the same solvent to remove any soluble impurities. Samples were deoxygenated with a nitrogen purge for 15 min and then sealed with a Teflon tape. The fluorescence of samples prepared using the two different methods was compared at room temperature and no significant deviations were found.

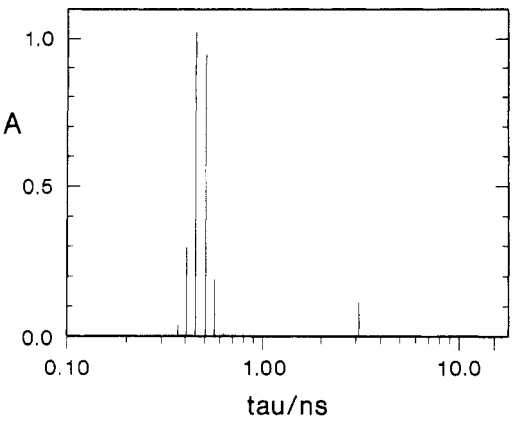

Figure 1. ESM analysis for the PAQ fluorescence lifetimes. The plots are of amplitude (A) of a lifetime component vs lifetime: PAQ in chloroform at 283 K, exponential analysis: $\tau_1 = 6.94$ ns, $\tau_2 = 0.51$ ns. ESM analysis: 70 exponential probe functions, τ/ns = 0.01–15.0, $\tau_1 \cong 3.1$, $\tau_2 \cong 0.49$.

The sample vial was installed in a cryostat, where the sample's temperasture was read out and controlled by a cryogenic thermometer/controller (CTI-cryogenics Model 4025); the absolute uncertainty in temperature was ±2.5 K.

Samples with lifetimes greater than 2 ns were excited with a hydrogen flash lamp. The excitation wavelength was adjusted to 418–420 nm by a monochromator. A monochromator was not used for the emission light since the fluorescence is weak; however, a Corning 2-58 glass cutoff filter (cutoff for $\lambda \leq 620$ nm) was used. Lifetimes less than 2 ns were measured using a pulsed laser. Both a monochromator set at 650 nm and a Corning 2-58 glass filter were used to exclude the strong scattered light in emission.

The pulsed laser consists of a cavity-dumped rhodamine-6G dye laser,[23] which is synchronously pumped by a mode-locked argon ion laser. The excitation wavelength was fixed at 570 nm. The number of data channels in the fluorescence profile is 256; usually 200 were used for analysis with 5000–10000 counts collected in the maximum-count channel. All the fluorescence lifetime analyses had values of χ^2 in the range 0.9–1.5 and residuals were random.

ϵ_s values vs temperature were obtained from the literature.[24] Refractive indices n from −10 to 30 °C were measured using a Bausch and Lomb Model refractometer. Both ϵ_s and n were fitted to curves versus temperature, from which the experimental ϵ_{op} ($=n^2$) and ϵ_s values were obtained by interpolation.

NMR spectra were measured on a Varian XL200 NMR spectrometer with a spectral width of 10 ppm.

Results and Discussion

1. Calculation of λ_{out}. The experimental temperature range for each solvent between the boiling point and the melting point is about 130 K. We assume that there is no significant change in the PAQ molecular conformation in each solvent with temperature.

In the analysis λ_{out} was calculated at each temperature from eq 4b with B estimated from eq 4a. With a_D, a_A, and r_{DA} taken as 7, 4, and 14 Å, respectively,[19] B is 1.80 eV. λ_{in} was taken to be temperature independent at 0.200 eV.[19]

2. Measurement of Fluorescence Lifetimes. The fluorescence lifetimes of PAQ and $PAQH_2$ were measured at different temperatures for six solvents. The data are given in Table I.[25] ET

(23) Ware, W. R.; Pratinidhi, M.; Bauer, R. K. *Rev. Sci. Instrum.* **1983**, *54*, 1148.

(24) (a) *Landolt-Bornstein*; Springer-Verlag: Berlin, 1959; Bd. 2, *Vol. 6* and *Vol. 8*. (b) Furutsuke, T.; Imura, T.; Kojima, T. *Technol. Rep. Osaka Univ.* **1974**, *24*, 367.

TABLE I: Fluorescence Lifetimes, Rate Constants, and Reorganization Energies as a Function of Temperature for PAQ and $PAQH_2$

solvent	T/K	ϵ_s[a]	ϵ_{op}[a]	λ[b]/eV	τ_1(PAQ)[c]/ns	τ_2($PAQH_2$)[c]/ns	k_{ET}[d]/10^9 s^{-1}
ethyl ether	293	4.38	1.8420	0.766	11.00	12.80	0.01278
	273	4.70	1.8726	0.778	11.71	12.89	0.00782
	260	5.03	1.8926	0.793	12.03	13.11	0.00685
	245	5.42	1.9157	0.808	12.42	13.17	0.00459
	200	6.83	1.9861	0.843	13.22	13.45	0.00129
	185	7.40	2.0099	0.852	13.34	13.50	0.00089
ethyl acetate	293	6.10	1.8835	0.861	10.17	11.41	0.0107
	280	6.41	1.9036	0.865	10.44	11.60	0.0096
	273	6.58	1.9041	0.872	10.60	11.72	0.0090
	260	6.89	1.9268	0.873	10.97	11.94	0.0074
	245	7.25	1.9444	0.877	11.38	12.29	0.0065
	200	8.33	1.9974	0.885	12.38	12.82	0.0028
acetonitrile	342	28.83	1.7406[e]	1.172	5.10	11.30	0.1076
	335	30.33	1.7493[e]	1.170	5.80	11.30	0.0839
	293	39.36	1.8010[e]	1.154	7.20	11.60	0.0527
	280	42.16	1.8171[e]	1.148	7.75	11.70	0.0436
	272	43.88	1.8271[e]	1.144	8.30	12.00	0.0371
	260	46.46	1.8420[e]	1.138	8.40	12.10	0.0364
	250	48.61	1.8545[e]	1.134	8.80	12.20	0.0317
	245	49.69	1.8613[e]	1.131	9.13	12.30	0.0282
chloroform	293	4.928	2.0965	0.693	0.48	9.05	1.98
	283	5.129	2.1031	0.705	0.52	9.49	1.81
	273	5.310	2.1090	0.715	0.45	9.16	2.13
	265	5.463	2.1140	0.722	0.54	9.46	1.74
	261	5.539	2.1165	0.725	0.55	9.50	1.70
	255	5.654	2.1203	0.731	0.52	9.96	1.84
	247	5.810	2.1254	0.737	0.68	9.41	1.36
methylene chloride	293	8.93	2.0340	0.857	1.47	8.85	0.57
	280	9.70	2.0457	0.867	1.60	9.05	0.51
	270	10.29	2.0547	0.874	1.65	9.05	0.50
	260	10.88	2.0637	0.879	1.66	8.60	0.49
	250	11.47	2.0727	0.884	1.79	8.90	0.45
	240	12.06	2.0818	0.888	1.84	9.0 ± 0.25	0.43 ± 6%
	230	12.65	2.0909	0.891	1.90	8.8 ± 0.2	0.41 ± 6%
2-methyltetrahydrofuran	293	7.009	1.9793	0.853	8.94	11.5 ± 0.5	0.024 ± 11%
	280	7.255	1.9854	0.859	9.35	10.80	0.015
	270	7.465	1.9901	0.863	9.68	11.2 ± 0.25	0.014 ± 6%
	260	7.699	1.9948	0.869	10.08	11.6 ± 0.25	0.013 ± 8%
	240	8.250	2.0043	0.880	10.48	11.9 ± 1	0.011 ± 8%
	230	8.578	2.0090	0.886	10.6	11.7	0.0090

[a] Data from ref 24, unless otherwise indicated. [b] λ was obtained from eqs 3 and 4b with λ_{in} = 0.200 eV and B = 1.80 eV. [c] Lifetimes have an error of ±0.1 ns unless otherwise indicated. [d] Error of $k_{ET}/10^9$ s^{-1} in chloroform is ±0.5, in methylene chloride is ±0.05, in all other solvents is ±0.005. Δk_{ET} was calculated from

$$\Delta k_{ET} = \frac{\partial k_{ET}}{\partial \tau_1}\Delta\tau_1 + \frac{\partial k_{ET}}{\partial \tau_2}\Delta\tau_2$$

with the maximum values $\Delta\tau = \Delta\tau_2$ = 0.10 ns. [e] Measured in our laboratory.

rate constants were calculated using eq 5.

As a check on our use of fluorescence lifetimes to calculate ET rate constants, we have used the exponential series method (ESM)[26] to analyze the two exponential lifetimes for PAQ in chloroform (see Figure 1). The ESM analysis shows clearly that the longer lifetime (assumed to arise from $PAQH_2$) has a very sharp distribution and is thus essentially almost conformation independent. However, the shorter lifetime (assumed to arise from PAQ) has a broader distribution. Since the longer lifetime component ($PAQH_2$) arises only from the porphyrin part of the molecule, which is in a planar conformation, it is reasonable that its lifetime appears as a sharp peak in the ESM spectrum. However, the PAQ lifetime is shortened by the intramolecular ET reaction, which involves both the porphyrin and quinone parts. Thus any distribution in the conformation of the PAQ molecule arising from the flexible amide linkage will lead to a distribution of lifetimes. Nevertheless, the lifetime at the ESM distribution peak (short lifetime) has virtually the same value as that obtained from the dual exponential analysis. Note that the shorter lifetime is assigned to PAQ and the longer lifetime to residual unoxidized $PAQH_2$. The fluorescence from the latter is very weak and cannot be measured accurately, since the data channels were set up for detecting 0–1 ns photons. Thus the large deviation of the longer lifetime is not significant.

From the above arguments we are justified in assuming that the shorter lifetime obtained from the dual exponential analysis corresponds to the lifetime of PAQ in its most probable conformation for ET to occur. We shall thus assume that any value of H_{rp} that we obtain from our analysis corresponds to that for the most probable conformation. We also assume that H_{rp} is temperature independent.

3. Solvent Dependence of the ET Rate Constants in PAQ. In our previous analysis[20] of the ET rate constants k_{ET} for PAQ, we rearranged eq 1 into a linearized form

$$\ln [k_{ET}\lambda^{1/2}] = C_1 - \frac{\Delta G^*}{k_B T} \qquad (6)$$

where

$$C_1 = \ln\left[\frac{2\pi}{\hbar}\frac{H_{rp}^2}{(4\pi k_B T)^{1/2}}\right]$$

(25) As seen in Table I, usually the PAQ samples exhibit two fluorescence lifetimes. The long-lifetime component is attributed to small amounts of $PAQH_2$ remaining in the sample and is usually of small amplitude compared to the short-lifetime component. Thus the longer lifetime is subject to considerable error. This is why we have only used the lifetimes measured for $PAQH_2$ samples for estimating τ_2.

(26) Siemiarczuk, A.; Wagner, B. D.; Ware, W. R. *J. Phys. Chem.* **1990**, *94*, 1661.

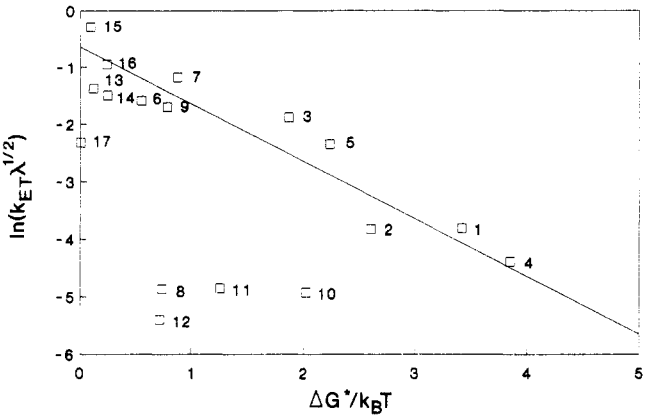

Figure 2. Marcus analysis of the solvent dependence k_{ET} for PAQ at 295 K in PAQ using eq 6 (adapted from ref 20). The solvent key is (1) acetonitrile; (2) proprionitrile; (3) benzonitrile; (4) acetone; (5) *n*-butyl alcohol; (6) 1,2-dichloroethane; (7) methylene chloride; (8) 2-methyltetrahydrofuran; (9) 1,1,1-trichloroethane; (10) 1,2-dimethoxyethane; (11) ethyl acetate; (12) ethyl ether; (13) chlorobenzene; (14) α-chloronaphthalene; (15) chloroform; (16) 1,2-dibromoethane; (17) anisole.

Thus a plot of ln $[k_{ET}\lambda^{1/2}]$ vs $\Delta G^*/k_BT$ should give a straight line with a slope of −1.00.

The Gibbs energy $\Delta G°$ of the ET reaction in PAQ can be calculated from

$$\Delta G° = \Delta G_{\pm} - \Delta U_{S_1} \tag{7}$$

where ΔU_{S_1} is the energy of the ^{1}P*AQ excited state, which is determined to be 1.90 eV from the overlap of the normalized absorption and fluorescence spectra[19] and assumed to be solvent and temperature independent. $\Delta G_{\pm}$ is the Gibbs energy of the radical ion pair state $P^{\bullet+}AQ^{\bullet-}$ relative to the ground state and can be determined in various solvents from

$$\Delta G_{\pm} = e(E°_{P^+/P} - E°_{Q/Q^-}) - \frac{e^2}{4\pi\epsilon_0\epsilon_s r_{PQ}} \tag{8}$$

where $E°_{P^+/P}$ and $E°_{Q/Q^-}$ are the standard reduction potentials of the porphine and the quinone, respectively, measured in the specific solvent, and r_{PQ} is the center-to-center distance between the porphine ring and the quinone ring. The second term in eq 8 is a Coulomb correction term.[20] The reduction potentials were measured (by Dr. P. Y. Gadzekpo in Dr. M. D. Archer's lab in Cambridge, England[20]) in each solvent, using differential pulse voltammetry.

It has been shown in paper 5[20] that, with $\Delta G°$ values calculated from eqs 7 and 8, the solvent dependence of the experimental k_{ET} rate constants can be correlated reasonably well with eq 6. However, as seen in Figure 2, there remains considerable scatter in the correlation.

4. Analysis of the Temperature Dependence of ET in PAQ. For our analyses of the temperature dependence of ET rate constants in PAQ we have used a modified form of eq 6

$$\ln [k_{ET}(\lambda T)^{1/2}] = C_2 - \frac{\Delta G^*}{k_B T} \tag{9}$$

where

$$C_2 = \ln \left[\frac{2\pi}{\hbar} \frac{H_{rp}^2}{(4\pi k_B)^{1/2}} \right]$$

A plot of ln $[k_{ET}(\lambda T)^{1/2}]$ vs $\Delta G^*/k_BT$ should also give a straight line with a slope of −1.00.

When we apply eq 9 with the assumption that both $\Delta G°$ and B are temperature independent for each solvent, the data for all solvents listed in Table II, except chloroform (vide infra), fall on linear plots with good correlation coefficients; however, the slopes vary from −2.12 to −0.82. One would expect that, in principle, both $\Delta G°$ and the B factor may be temperature dependent. The former is affected by the solvation entropy; the latter can be affected by changes in the average molecular conformation. However, the range of conformation change in PAQ is very limited; i.e., the extended and compacted conformations only change r_{DA} from 12.4 to 14.6 Å,[18] which by eq 3b only allows the B factor to vary from 1.67 to 1.91. We thus arbitrarily assume that B is temperature indepedent[27] and has the value $B = 1.80$ ($r_{DA} \cong 14$ Å). We further assume that $\Delta G°$ depends linearly on T, that is

$$\Delta G°(T) = \Delta G°(293) + K(T - 293) \tag{10}$$

By adjusting the coefficient K for each solvent we can force the slope of plots of eq 9 to be −1.00. This analysis is given in Table II. The $\Delta G°$ change required with temperature in all solvents is modest (total change over the full temperature range ≤ 0.12 eV), which is consistent with other studies.[11,28,29] It is interesting that all the K values are negative; this implies that $\Delta S°$ is positive.

TABLE II: Marcus Analysis of the PAQ Temperature Dependence of k_{ET} According to Eq 9

solvent	slope	intercept	K^a/meV K^{-1}	r^b
ethyl ether[c]	−1.00	−2.00	−1.06	0.996
ethyl acetate	−1.00	−1.40	−0.62	0.998
acetonitrile	−1.00	2.55	−0.56	0.988
chloroform				*d*
methylene chloride	−1.00	2.13	0.00	0.960
2-methyltetrahydrofuran	−1.00	−1.48	−0.93	0.914

[a] K is a parameter in eq 10 that is adjusted until the slope of a least-squares fit to eq 9 is −1.00. [b] Absolute value of the correlation coefficient. [c] $\Delta G°$ in ethyl ether is not known; however, it was set to the same valueas in ethyl acetate, since these two solvents have similar ϵ_s and k_{ET} values. [d] Close to the inverted region; the data cannot be analyzed by eq 6. k_{ET} is virtually temperature independent (see Table I).

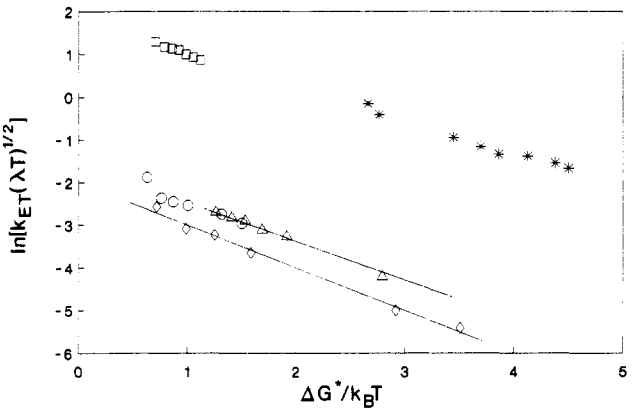

Figure 3. Marcus analysis of the temperature dependence of k_{ET} using eq 9: □, methylene chloride; ◇, ethyl ether; ○, 2-MTHF; △, ethyl acetate; *, acetonitrile.

5. The Electronic and Nuclear Factors. The temperature dependence of the electronic factor κ_{el} is expected to be very small, while that of the nuclear factor should be pronounced. Thus a temperature dependence experiment allows these two factors to be separated. This can be seen clearly from Figure 3, which is a composite plot of eq 9 for all solvents listed in the tables except chloroform. The ordinate is ln $[k_{ET}(\lambda T)^{1/2}]$ and the abscissa is $\Delta G^*/k_BT$. The intercept of each line should be C_2 (eq 9). Thus from the intercepts we obtain an estimate of κ_{el} and the electronic coupling energy H_{rp}. Derived values of H_{rp}, κ_{el}, and κ_n are listed in Table III.

The variation of κ_{el}, and hence H_{rp}, among all the solvents studied is quite large. The H_{rp} values appear to be correlated with

(27) B probably has some small temperature dependence, especially as we find that the conformation of PAQ changes with solvent (vide infra); however, we believe that ascribing the variation in slopes to a temperature dependence of $\Delta G°$ is more reasonable.

(28) Oevering, H.; Paddon-Row, M. N.; Heppener, M.; Oliver, A. M.; Cotsaris, E.; Verhoeven, J. W.; Hush, N. S. *J. Am. Chem. Soc.* **1987**, *109*, 3258.

(29) Gunner, M. R.; Robertson, D. E.; Dutton, P. L. *J. Phys. Chem.* **1986**, *90*, 3783.

TABLE III: Parameters Obtained from the Temperature Studies

solvent	ϵ_s[a]	k_{ET}[a]/10^9 s^{-1}	$\Delta G°$/eV	λ[b]/eV	H_{rp}[c]/meV	κ_{el}[d]/10^{-6}	κ_n[e]
ethyl ether	4.4	0.0128	−0.53	0.766	0.0343	3.7	0.487
chloroform	4.9	1.98	−0.77	0.693	(0.293)[f]	286	0.919
ethyl acetate	6.1	0.0107	−0.53	0.861	0.0462	6.4	0.284
2-methyltetrahydrofuran	7.0	0.024	−0.62	0.853	0.0444	5.8	0.533
methylene chloride	8.9	0.57	−0.61	0.857	0.269	217	0.494
acetonitrile	39.4	0.0527	−0.52	1.154	0.332	285	0.032

[a] Values measured at 293 K. [b] Values calculated at 293 K (eqs 3 and 4 with λ_{in} = 0.200 eV). [c] Calculated from C_2 (eq 9) and the intercepts in Table II. [d] $\kappa_{el} = [(2\pi/\hbar)H_{rp}^2/(4\pi\lambda k_B T)^{1/2}]/(k_B T/h)$, calculated for T = 293 K. [e] $\kappa_n = \exp[-(\Delta G° + \lambda)^2/(4\lambda k_B T)]$, calculated for T = 293 K. [f] Value determined from eq 1 assuming $\Delta G^* = 0$.

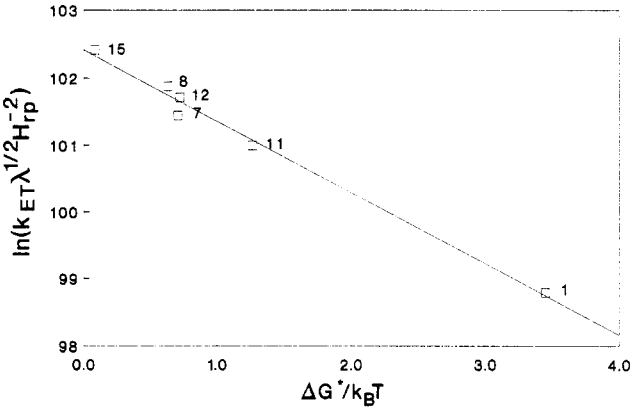

Figure 4. Analysis of k_{ET} for PAQ according to eq 11. The solvent key is the same as for Figure 2.

the solvent dielectric constant. In the PAQ molecule both the porphine and quinone are hydrophobic groups; in polar solvents these two moieties may tend to form a more compact structure where the D–A distance is smaller and hence H_{rp} should be larger. In nonpolar solvents the PAQ molecule is likely to adopt a more extended conformation where the D–A distance is larger and hence H_{rp} should be smaller, yielding smaller k_{ET} values. This hypothesis is confirmed by NMR epxeriments described below. The H_{rp} values in methylene chloride and chloroform are anomalously high, compared to the other solvents with low dielectric constants. We believe that this is due to a heavy atom effect that we shall explore in a later paper.[30]

The κ_n values are also slightly solvent dependent (Table III); however, there does not appear to be any consistent trend with dielectric constant, except that κ_n is smallest for acetonitrile, the solvent with the largest dielectric constant.

In the previous analysis[20] of the solvent dependence of k_{ET} in PAQ, H_{rp} was assumed to be independent of solvent and was taken to have the value in acetonitrile. However, as seen in Figure 2, a plot of ln $(k_{ET}\lambda^{1/2})$ versus $\Delta G^*/k_B T$ is rather scattered. If we now use the H_{rp} values determined for the different solvents (including chloroform, see below) and reanalyze our earlier data[20] according to eq 11, the scattered points in Figure 1 (for which we have temperature dependence measurements) all fit on a line with a slope near −1.00 (see Figure 4).

$$\ln (k_{ET}\lambda^{1/2}H_{rp}^{-2}) = C_3 - \Delta G^*/k_B T \qquad (11)$$

where

$$C_3 = \ln\left[\frac{2\pi}{\hbar(4\pi k_B T)^{1/2}}\right]$$

A least-squares fit to eq 11 gives a slope of −1.06 ± 0.06 and intercept 102.41 ± 0.15 (which is very close to the value of C_3 = 102.3 calculated from the physical constants for T = 293 K) with a correlation coefficient r = 0.989. This analysis is consistent with our interpretation that the low points for 2-methyltetrahydrofuran, ethyl ether, and ethyl acetate in Figure 3 arise almost entirely from small H_{rp} values.

(30) Liu, J.-Y.; Bolton, J. R., unpublished work.

TABLE IV: Experimental Chemical Shifts δ (ppm) of the Phenyl Protons in $PAQ(Me)_2$ and ADB

	DMSO-d_6/CD_3CN[a]	DMSO-d_6	DMSO-d_6/$CDCl_3$[a]
$PAQ(Me)_2$	6.131–5.925	6.139–5.957	6.240–6.065
ADB	6.902–6.743	6.781–6.636	6.00–5.885
$\Delta\delta$	−0.77	−0.64	+0.22

[a] Ratio 0.7:0.3 by volume.

6. Inverted Region. $|\Delta G°|$ for the ET reaction of PAQ in chloroform is close to the value of the reorganization energy (see Table III). The reaction is thus near the turning point beyond which the system goes into the inverted region; indeed, as expected when $\Delta G^* \cong 0$, the rate constants in chloroform are almost temperature independent. Although the applicability of eq 1 near the inverted region may be questionable, we may nevertheless get an estimate of H_{rp} in chloroform by assuming that $\Delta G^* = 0$ (see Table III).

7. Solvent Dependence of NMR Spectra. Our temperature-dependent ET experiments have shown that the H_{rp} values change over a large range in different solvents; this can be caused by a molecular conformation change that can affect the distances between the donor and the acceptor.

The solvent polarity dependence of the D–A distance can be examined by an analysis of NMR spectral data. In the PAQ molecule the 18 π electrons in the porphyrin moiety circulate in the plane and give rise to an enhanced diamagnetic susceptibility in the perpendicular direction. This magnetic shell affects the chemical shift of the surrounding atoms. Protons at the top or inside of the porphyrin ring are subjected a shielding effect, such that their chemical shift moves upfield in the NMR spectrum; while protons outside the porphyrin ring are subjected to a deshielding effect and shift downfield in the NMR spectrum.[31,32] From this effect, we can estimate the change of the D–A distance in PAQ in different solvents from changes in the chemical shifts of the acceptor protons in the NMR spectrum.

Since the PAQ samples always have a residual of $PAQH_2$ present, which would complicate the NMR analysis, we chose a porphyrin linked to a dimethoxybenzene moiety $PAQ(Me)_2$ instead of PAQ to avoid any conformation problems that the hydroxy groups can produce by the formation of hydrogen bonds. Acetyl-*N*-dimethoxybenzylamine (ADB) was chosen as a reference compound, in which a methyl group replaces the tetratolylporphyrin group. The NMR spectra of $PAQ(Me)_2$ and ADB

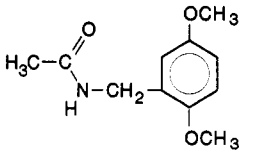

ADB

were measured in DMSO-d_6, DMSO-d_6/$CDCl_3$ (0.7:0.3) and DMSO-d_6/CD_3CN (0.7:0.3) separately. In polar solvents the chemical shifts of the phenyl protons on the dimethoxybenzene

(31) Bovey, F. A. *NMR Spectroscopy*, 2nd ed.; Academic Press: New York, 1988; pp 108–114.

(32) Lenden, D. E.; Cox, R. H. *Analytical Applications of NMR Chemical Analysis*; Wiley: New York, 1977; Vol. 48, pp 31–33.

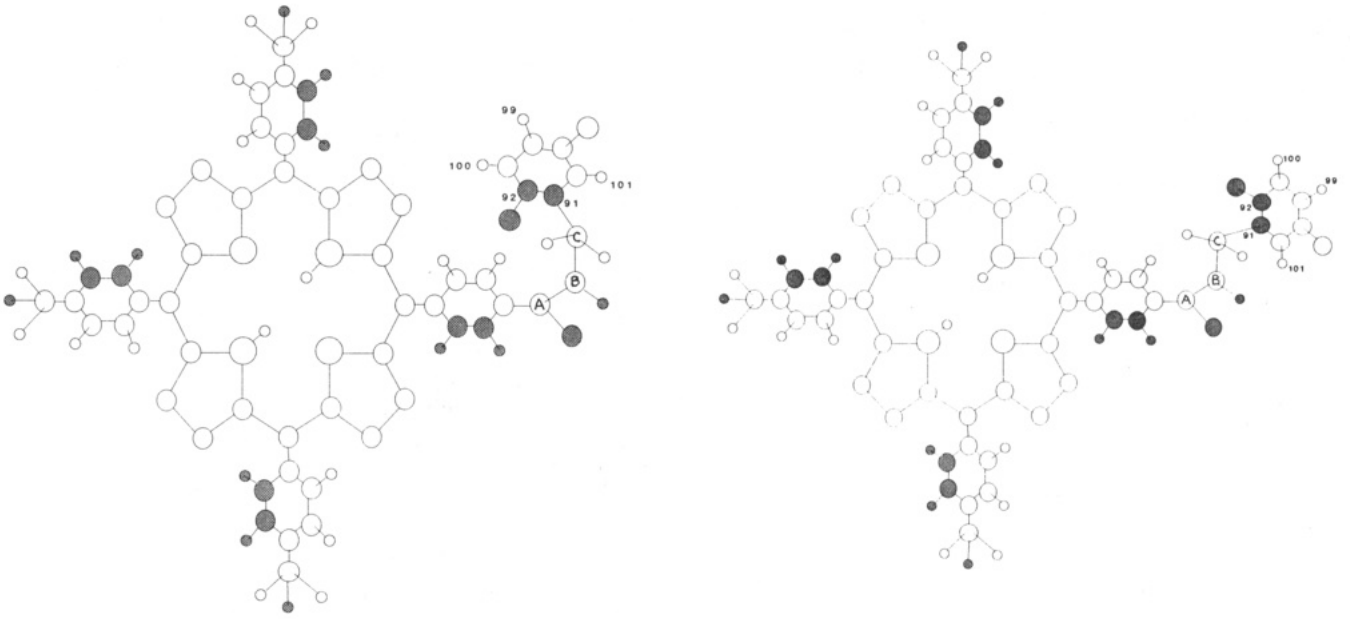

Figure 5. Molecular conformation of PAQ when (a, left) $\pi(91) = 90°$, $\pi(92) = 275°$; (b, right) $\pi(91) = 180°$, $\pi(92) = 0°$.

TABLE V: Results of Calculations Using the XYZSHIFT Program

	atom no	$\Delta\delta$,[a] ppm	distance of the[b] center of the dimethoxybenzene to the porphyrin center/Å
$\pi(91) = 90°$	99	−0.0123	7.46
$\pi(92) = 275°$	100	−0.0205	9.72
	101	−0.8844	7.77
$\pi(91) = 180°$	99	0.0285	14.21
$\pi(92) = 0°$	100	0.230	13.24
	101	0.1674	11.53

[a] Chemical shift change, calculated using the XYZSHIFT program with parameters as defined in the text. [b] Using a molecular simulation computer model, Schmidt et al.[18] have calculated that this distance is 12.4 Å in the compact conformers and 14.6 Å in the extended conformers.

moiety in the PAQ(Me)$_2$ molecule are smaller than those for the corresponding protons in ADB. In nonpolar solvents a downfield chemical shift is observed for these phenyl protons (see Table IV).

Gust et al.[33] have developed a program called XYZSHIFT, which can calculate the chemical shifts of protons in a porphyrin-containing molecule according to their distances from the porphyrin center. By using their program, we were able to determine in which solvents the average r_{DA} distance is smaller.

The bond distances and angles for the porphine and quinone moieties of PAQ were taken from the crystal structure data of tetraphenylporphine[34] and *p*-benzoquinone.[35] Each atom's position was defined by bond length, bond angle and dihedral angle. The XYZSHIFT program transfers the positions into Cartesian coordinates and calculates each proton's NMR chemical shift.

In PAQ the bridge connecting the porphyrin and quinone is a peptide bond. There is a hydrogen bond connecting N–H and C=O groups, and the lone pair electrons on the nitrogen have to conjugate with the benzoyl π electrons; these interactions make part of the bridge rigid. The only factor that allows flexibility of conformation is the methylene group. By changing the dihedral angle of the 91st atom (the angle between bond A–B and bond C–91; see Figure 5), a folded (π = 60–120° or 300–360°) or extended (π = 120–300°) conformation of PAQ can be reached. Also by changing the dihedral angle of the 92nd atom (the angle between bond B–C and bond 91–92) the relative orientation of the porphyrin plane and the quinone plane can be changed. By changing the two dihedral angles, we have found that only when $\pi(91)$ = 90–120° can the phenyl protons in the acceptor have upfield shifts (the data are shown in Table V). We have found that when $\pi(91) = 90°$, $\pi(92) = 275°$, the three quinone protons all have upfield shifts. When $\pi(91) = 180°$, $\pi(92) = 0°$, the three quinone protons have downfield shifts. The molecular conformations of these two situations are shown in Figure 5.

In the calculations we did not consider the internal molecular torsion or conformational hindrance, so the distances between donor and acceptor in the folded conformation are smaller as compared to the result of an earlier calculation;[18] however, our result does show that when the molecule is more compacted, the NMR lines should move upfield; this is the situation observed in polar solvents. When the molecule is more extended, the NMR lines move downfield; and this is the situation observed in nonpolar solvents. Although we did not measure the fluorescence lifetimes of PAQ in DMSO, this analysis nevertheless shows that in polar solvents PAQ has a smaller average r_{DA} and hence should have larger H_{rp} values. This implies that H_{rp} is derived, at least in part, from "through solvent" interactions. We have presented evidence for this mechanism in another study.[21]

Conclusions

By analyzing the temperature dependence of k_{ET} in PAQ in several solvents we have been able to separate the electronic and nuclear factors. We thus have shown that H_{rp} is solvent dependent, being larger in polar solvents and smaller in nonpolar solvents. This solvent dependence of H_{rp} is largely responsible for the scatter in a previous attempt to fit the solvent dependence of k_{ET} to the Marcus equation (eq 1). By analysis of NMR spectra we have shown that the average conformation of the PAQ molecule is more compacted in polar solvents and extended in nonpolar solvents. This is a possible reason for the solvent dependence of H_{rp}.

Acknowledgment. This research was supported by an Operating Grant from the Natural Sciences and Engineering Research Council of Canada. We thank Prof. W. R. Ware for the use of his fluorescence lifetime apparatus, Prof. D. Gust for giving us the XYZSHIFT program, Dr. A. Siemiarczuk for helping to set up the laser apparatus, and Dr. M. D. Archer for her helpful comments. Finally, we thank the two referees for their detailed reading

(33) (a) Gust, D.; Moore, T. A.; Liddell, P. A.; Nemeth, G. A.; Makings, L. R.; Moore, A. L.; Barrett, D.; Pessiki, P. J.; Bensasson, R. V.; Rougeé, M.; Chachaty, C.; De Schryver, F. C.; Van der Auweraer, M.; Holzwarth, A. R.; Connolly, J. S. *J. Am. Chem. Soc.* **1987**, *109*, 846. (b) Chachaty, C.; Gust, D.; Moore, T. A.; Nemeth, G. A.; Liddell, P. A.; Moore, A. L. *Org. Magn. Reson.* **1984**, *22*, 39.

(34) Pearson, W. B.; Calvert, L. D.; Trotter, J.; Trotter, J. *Struct. Rep.* **1964**, *29*, 617.

(35) Pearson, W. B.; Calvert, L. D.; Trotter, J.; Trotter, J. *Struct. Rep.* **1964**, *24*, 639.

of the manuscript and their excellent suggestions, which improved the paper considerably.

Registry No. PAQ, 98330-76-8; $PAQ(Me)_2$, 98330-78-0; acetonitrile, 75-05-8; propionitrile, 107-12-0; benzonitrile, 100-47-0; acetone, 67-64-1; *n*-butyl alcohol, 71-36-3; 1,2-dichloroethane, 107-06-2; methylene chloride, 75-09-2; 2-methyltetrahydrofuran, 96-47-9; 1,1,1-trichloroethane, 71-55-6; 1,2-dimethoxyethane, 110-71-4; ethyl acetate, 141-78-6; ethyl ether, 60-29-7; chlorobenzene, 108-90-7; α-chloronaphthalene, 90-13-1; chloroform, 67-66-3; 1,2-dichloromethane, 106-93-4; anisole, 100-66-3.

Modeling the Oscillatory Bromate Oxidation of Ferroin in Open Systems

Sándor Kéki,† István Magyar,† Mihály T. Beck,*,† and Vilmos Gáspár*,†,‡

Department of Physical Chemistry, Kossuth Lajos University, 4010 Debrecen, P.O. Box 7, Hungary and Department of Chemistry, West Virginia University, Morgantown, West Virginia 26506-6045
(Received: May 9, 1991; In Final Form: October 22, 1991)

A model for the ferroin–bromate–bromide–sulfuric acid system in a continuously stirred (flow-through) tank reactor has been constructed by extending the Noyes–Field–Thompson mechanism with the following *composite processes*: (a) ferroin–bromate, (b) ferroin–bromous acid, (c) ferroin–hypobromous acid, (d) ferroin–bromine, (e) ferriin–bromide, and (f) ferriin–bromine. The calculated high-amplitude oscillations and kinetic phase diagram are in good accordance with the experiments reported earlier. By completing the scheme with a reaction step accounting for the precipitation and dissolution of a ferroin–tribromide salt, the batch oscillations found at high concentrations of reactants can also be simulated.

Introduction

The Belousov–Zhabotinsky (BZ) oscillatory reaction, the cerium(III)-catalyzed oxidation of malonic acid by acidic bromate, has been commonly applied during the last few decades for studying a wide variety of temporal and spatial instabilities in chemical systems.[1-4]

A small amount of tris(1,10-phenanthroline)iron(II), a well-known redox indicator called ferroin, is often added to a BZ mixture in order to better visualize the periodic changes. Vavilin et al.[5] observed first that ferroin itself can also catalyze the BZ reaction. Later, Beck et al.[6] found that even the simple ferroin–bromate batch reaction can oscillate at extremely high concentrations of reactants. Another necessary condition for the periodic behavior is the continuous but partial removal of the produced bromine by an inert gas stream. The cerium–bromate batch reaction shows no periodicity under the same conditions. This difference in behavior of the ferroin- and cerium–bromate systems has never been explained in terms of mechanisms. The ferroin–bromate reaction is bistable in a continuously stirred (flow-through) tank reactor (CSTR). Oscillations can emerge only by adding bromide ion to the input flow.[7] The bromide ion-controlled oscillations are similar to those observed in the analogous cerium system in a CSTR.[8,9] However, some characteristic features of oscillations in the ferroin system are different from those in the cerium system, for example, (1) During an oscillatory cycle, the total amount of ferroin is oxidized to ferriin, the iron(III) complex, and vice versa. It results in a periodic color change from red to blue and back to red, respectively. Accordingly, high-amplitude potential oscillations can be detected by a platinum electrode in phase with the color change. The cerium–bromate–bromide system possesses only small-amplitude oscillations.[8,9] (2) Oscillations occur in a much broader range of input concentrations in the ferroin-containing system than in that found with cerium.[8,9]

One may think that the acidic bromate oxidation of cerium(III) or ferroin should proceed by similar mechanisms. In this case, the ferroin system could easily be simulated on the basis of the well-established mechanism for the cerium system. Thus, one should simply change the rate constants of a few elementary steps in accordance with the different redox properties of the two catalysts. On the contrary, we failed to characterize the ferroin system within the framework of the Field–Körös–Noyes (FKN)[10] theory for the cerium-catalyzed reaction.

TABLE I: A Model for the Ferroin–Bromate Reaction[a]

$BrO_3^- + Br^- + \{2H^+\} \rightleftharpoons HOBr + HBrO_2$	(1)
$HBrO_2 + Br^- + \{H^+\} \rightleftharpoons 2HOBr$	(2)
$HOBr + Br^- + \{H^+\} \rightleftharpoons Br_2 + \{H_2O\}$	(3)
$BrO_3^- + HBrO_2 + \{H^+\} \rightleftharpoons 2BrO_2^\bullet + \{H_2O\}$	(4)
$2HBrO_2 \rightleftharpoons HOBr + BrO_3^- + \{H^+\}$	(5)
$Fe(phen)_3^{2+} + BrO_2^\bullet + \{H^+\} \rightarrow Fe(phen)_3^{3+} + HBrO_2$	(6)
$2Fe(phen)_3^{2+} + BrO_3^- + \{3H^+\} \rightarrow 2Fe(phen)_3^{3+} + HBrO_2 + \{H_2O\}$	(7)
$2Fe(phen)_3^{2+} + HBrO_2 + \{2H^+\} \rightarrow 2Fe(phen)_3^{3+} + HOBr + \{H_2O\}$	(8)
$2Fe(phen)_3^{2+} + HOBr + \{H^+\} \rightarrow 2Fe(phen)_3^{3+} + Br^- + \{H_2O\}$	(9)
$2Fe(phen)_3^{2+} + Br_2 \rightarrow 2Fe(phen)_3^{3+} + 2Br^-$	(10)
$2Fe(phen)_3^{3+} + 2Br^- \rightarrow 2Fe(phen)_3^{2+} + Br_2$	(11)
$Fe(phen)_3^{3+} + Br_2 \rightarrow \{[Fe(phen)_3Br_2]^{3+}\}$	(12)
$Br_2 \rightarrow \{Br_2(gas)\}$	(13)

[a] Changes in the concentrations of species in brackets are not taken into account; phen = 1,10-phenanthroline.

The standard reduction potential of the ferriin/ferroin couple (1.06 V)[11] is lower than that of cerium(IV)/cerium(III) in sulfuric acid (1.44 V).[12] Therefore, it has been speculated in several reports[12-19] that ferroin, unlike cerium(III), could directly be

* Author to whom correspondence should be addressed.
† Kossuth Lajos University.
‡ West Virginia University.

(1) Belousov, B. P. *Ref. Radiat. Med.* **1959**, *1958*, 145.
(2) Zhabotinsky, A. M. *Dokl. Akad. Nauk SSSR* **1964**, *157*, 392.
(3) Zhabotinsky, A. M. *Concentration Selfoscillations*; Nauka: Moscow, 1974.
(4) Field, R. J.; Burger, M. *Oscillations and Traveling Waves in Chemical Systems*; Wiley: New York, 1985.
(5) Vavillin, V. A.; Gulak, P. V.; Zhabotinsky, A. M.; Zaikin, A. N. *Izv. Akad. Nauk SSSR, Ser. Khim.* **1969**, *11*, 2618.
(6) Beck, M. T.; Bazsa, G.; Hauck, K. *Ber. Bunsen-Ges. Phys. Chem.* **1980**, *84*, 408.
(7) Gáspár, V.; Bazsa, G.; Beck, M. T. *J. Phys. Chem.* **1985**, *89*, 5495.
(8) Orbán, M.; DeKepper, P.; Epstein, I. R. *J. Am. Chem. Soc.* **1982**, *104*, 2657.
(9) Geiseler, W. *Ber. Bunsen-Ges. Phys. Chem.* **1982**, *86*, 721.
(10) Field, R. J.; Körös, E.; Noyes, R. M. *J. Am. Chem. Soc.* **1972**, *94*, 8649.
(11) Schilt, A. A. *Analytical Applications of 1,10-phenanthroline and related compounds*; Pergamon: Oxford, U.K., 1969.
(12) Noyes, R. M. *J. Am. Chem. Soc.* **1980**, *102*, 4644.
(13) Yatsimirskii, K. B.; Tikhonova, L. P. *Coord. Chem. Rev.* **1985**, *63*, 241.
(14) Ganapathisubramanian, N.; Noyes, R. M. *J. Phys. Chem.* **1982**, *86*, 5158.

0022-3654/92/2096-1725$03.00/0